Development of an Anti-Aβ Monoclonal Antibody for In Vivo Imaging of Amyloid Angiopathy in Alzheimer's Disease

Robert P. Friedland,[*,1] *Ronald E. Majocha,*[2] *John M. Reno,*[3] *Leon R. Lyle,*[4] *and Charles A. Marotta*[2]

[1]*Department of Neurology, Case Western Reserve University, Cleveland, OH;*
[2]*Neurobiology Laboratory, Massachusetts General Hospital, Boston, MA,*
and Department of Psychiatry, Brown University, Providence, RI;
[3]*NeoRx Corp., Seattle, WA; and* [4]*Mallinckrodt Medical, Inc., St. Louis, MO*

Abstract

We evaluated the efficacy of murine monoclonal antibodies (MAbs) targeted to the Aβ amyloid of Alzheimer's disease for development of procedures for the in vivo identification of amyloid angiopathy (AA). MAbs to Aβ were prepared and screened for effectiveness in visualizing AA and neuritic plaques in postmortem AD brain sections. They were assessed again after enzymatic cleavage to produce Fab fragments and after labeling with technetium-99m (^{99m}Tc) using a diamide dimercaptide ligand system. Modified and radiolabeled Fab fragments retained activity and specificity toward amyloid-laden blood vessels and neuritic plaques. A highly specific murine MAb, 10H3, was identified and characterized that fulfills criteria necessary for the development of an in vivo diagnostic imaging agent. Toxicity studies in rats showed the MAb to be safe. Biodistribution studies in mice demonstrated desirable properties for use as an imaging agent. Expansion and adaptation of these strategies may provide the methods and materials for the noninvasive analysis of AA in living patients, and permit assessment of the contribution of AA to the clinical and pathological features of AD.

Index Entries: Alzheimer's disease; amyloid angiopathy: in vivo diagnosis; monoclonal antibodies; single photon emission tomography.

Introduction

The brain circulation is involved in the pathological processes of Alzheimer's disease (AD). Nevertheless, the role of cerebrovascular lesions in the pathophysiology of the disease remains unknown (12). Amyloid angiopathy (AA) has been recognized since the early work of Scholz as a significant aspect of the microscopic pathology of AD (3). Although found to a lesser extent in some healthy older people, AA is severe and common in AD and occurs in greater than 90% of affected brains (4–7). The amyloid is readily demonstrated by application of Thioflavin S or Congo red to brain sections (5,6,8,9). These staining properties reflect the presence of twisted beta fibrils in the vessel wall (6).

---

*Author to whom all correspondence and reprint requests should be addressed: CWRU, Dept. of Neurology, 2074 Abington Rd., Cleveland, OH 44106.

Amyloid infiltration is widespread in the brain microvasculature: affected vessels often pass from the leptomeninges into the cortex. Small cerebral vessels with arterioles that appear as thickened tubes are observed. Involved vessels include small pial and intracortical arterioles, leptomeningeal vessels and, at times, intracortical capillaries, sometimes with destruction of the endothelium *(2–4)*. Immunocytochemical and electron microscopic studies indicated that the amyloid component of senile plaques often occurs in close proximity to affected microvessels *(5,11)*. However, AA may occur without senile plaques *(12)*, and the spatial association between plaques and AA may be a chance relationship.

Brain imaging has been widely used in the investigation of AD. However, at present neuroimaging cannot be used to make the diagnosis noninvasively. Furthermore, there are currently no mechanisms for the assessment of the disease's basic pathological features during life in the absence of surgery. The presence of amyloid deposits in small brain vessels in close proximity to the lumen *(11,12)* suggests that an intravenously administered radiolabeled antibody would be capable of in vivo localization. With the goal of developing a highly specific and reactive immunologic probe for AA, a series of studies were carried out on MAbs made to a sequence homologous to the Aβ peptide *(13)*. The peptide is the major protein component of amyloid deposits in the AD brain *(13)*. We identified and characterized a murine MAb, 10H3, that retains high reactivity and specificity toward AA after a series of modifications required to produce an imaging agent. Aspects of this work have been previously presented and published *(14)*.

Materials and Methods

Postmortem Brain

Postmortem brain material was obtained from the Brain Tissue Resource Center at McLean Hospital, Belmont, MA. The brain used for evaluating 10H3 was an 88-yr-old male with the clinical diagnosis of familial AD. The diagnosis was confirmed after postmortem examination, which demonstrated the widespread occurrence of senile plaques and neurofibrillary tangles in all brain areas examined. In addition, congophilic angiopathy was noted to involve intraparenchymal vessels as well as vessels within the subarachnoid space. The neurologically normal control brain used

in the present study was that of a 65-yr-old male. Brain sections failed to stain with Thioflavin S.

Preparation and Characterization of the Synthetic Amyloid Polypeptide

A 28 residue polypeptide homologous to Aβ was synthesized by Biosearch (San Rafael, CA). Amino acid analysis verified the structure. The amino acid sequence was reported by Masters and coworkers *(13)* and is here referred to as Aβ (1–28). Aβ (1–28) is homologous, but nonidentical, to the site occupied by amyloid precursor protein (APP) amino acids 597–624. Peptide samples were stored as a dry powder at –20°C until used.

Immunological Procedures

Immunocytochemistry

The preparation of MAb 10H3 was detailed in an earlier report *(15)*. Formalin fixed human postmortem brain tissue was kept in 30% sucrose overnight and serially sectioned on a cryostat at 40 μm. After storage in glycerol/water (1:1) -1% sodium azide at –20°C, they were rinsed in Tris-buffered saline (TBS) (0.9% NaCl, 20 mM Tris, pH 7.4), immersed in 1% H_2O_2 in TBS for 30 min and then rinsed in TBS. Each section was placed in a solution of the primary antibody, appropriately diluted in immunocytochemistry primary buffer (IPB) (10% goat serum, 2% BSA in TBS [TBS + 0.5% Triton X-100]) overnight. After rinsing with TBST, sections were treated with biotinylated goat antimouse IgG (Jackson ImmunoResearch Laboratories), diluted 1:200 in immunocytochemistry secondary buffer (ISB) (2% BSA in TBST) for 2 h and then rinsed with TBST. Sections were combined with Avidin DH: biotinylated horseradish peroxidase H complex (Vector) according to the manufacturer's directions, diluted with ISB, rinsed in TBST, developed for 2 min in a diaminobenzidine tetrahydrochloride solution, and mounted and coverslipped.

For the immunofluorescence procedure, the secondary antibody was rhodamine-conjugated goat antimouse IgG (Cappel), diluted 1:50, for 1 h in ISB. Photographs were taken with a Zeiss photomicroscope equipped with the appropriate excitation and barrier filters.

Dot Blots

Fab preparations were characterized on nitrocellulose blots of the starting antigen. Two micrograms of Aβ (1–28) peptide was spotted for each antibody and the latter were tested at concentrations rang-

ing from 0.05–0.2 µg/mL. The procedures were described in detail earlier (15).

Quantitation of Immunostained Plaques

A quantitative assay for antibody specificity was carried out on sections of AD cortex. The numbers of immunostained plaques were counted using a scored grid inserted into the microscope eyepiece. Each grid was 0.25 mm per side; 319 adjacent grids were counted per tissue section for a total area of 19.94 mm^2.

Antibody Purification

For studies on the purified antibody the latter was obtained from mouse ascites fluid in a single step using Protein G Sepharose Fast Flow (Pharmacia, Uppsala, Sweden) following the manufacturer's instructions. The purified IgG was characterized by isoelectric focusing as follows.

Isoelectric Focusing

Reagents were obtained from Pharmacia and were applied by means of the general directions supplied by the manufacturer ("Electrophoresis Catalogue").

Antibody Subclass Determination

Isotyping was performed on the purified samples using an ELISA assay for murine IgM, IgG, IgG$_2$a, and IgG$_3$ heavy chains and for kappa and lambda light chains. The procedure involved coating a 96-well microtiter plate with GAM (goat antimouse) iso-specific capture antibodies (Fisher Biotek) in phosphate buffered saline (PBS) overnight. Any unbound antibodies were removed by washing with 0.5% Tween-20 in PBS. Control and test samples were added at 1 µg/mL in CSPT buffer (5 chicken serum, 0.5% Tween-20 in PBS) and the plates were incubated at 4°C for 1 h. Unbound antibody was removed by washing with 0.5% Tween-20 in PBS before adding GAM IgG (pan-reactive) horseradish peroxidase conjugate (Fisher Biotek) and incubated again at 4°C for 1 h. The microtiter plate was washed again with 0.5% Tween-20 in PBS and a chromogenic substrate (ABTS [2,2'azino-bis (3-ethylbenzthiazoline-6-sulfonic acid] + H$_2$O$_2$, Sigma) was added for 30 min at room temperature. Optical densities were recorded on a dual-beam microtiter plate reader set at 415 nm (sample) and 490 nm.

Antibody Fragmentation

Fab fragments of 10H3 were obtained after enzymatic digestion of the whole antibody. Papain bound to agarose beads was obtained from Pierce and activated according to the manufacturer's instructions. 10H3 was exchanged into digestion buffer (0.02M sodium phosphate, pH 8.5, 0.003M EDTA, 0.02M L-cysteine), and adjusted to 5 mg/mL. Antibody was mixed with activated papain beads in a ratio of 1 mg of protein/0.05 mL packed volume of beads. After 18 h mixing at 37°C, the mixture was centrifuged and the supernatant applied to a 5 mL column of Q Sepharose Fast Flow (Pharmacia) equilibrated with 0.1M sodium phosphate, pH 8.5. The flow-through volume containing pure 10H3 Fab was collected and concentrated to 20 mg/mL. The Fab fragment was pure as judged by SDS-PAGE and gel filtration HPLC.

Radiolabeling of 10H3 Fab with ^{99m}Tc

The Fab fragment was radiolabeled with generator-produced ^{99m}Tc using the diamide dimercaptide bifunctional chelating agent, and procedures, described by Kasina and coworkers (16). Briefly, generator produced ^{99m}Tc pertechnetate was reduced by stannous ion and complexed gluconate with sodium. The reduced ^{99m}Tc gluconate was added to an acidified solution containing the diamide dimercaptide ligand. The ^{99m}Tc was trans-chelated into the ligand during a 15 min incubation at 75°C. The ^{99m}Tc ligand solution was cooled to room temperature and adjusted to pH 9.5 with bicarbonate buffer. A solution of antibody in phosphate-buffered saline was added to the ^{99m}Tc ligand solution and incubated at room temperature for 20 min. The ^{99m}Tc labeled antibody was then purified by anion exchange chromatography and diluted with normal saline prior to further use.

Toxicity, Biodistribution, and Flow Cytometry Studies

Toxicity studies were performed in adult Sprague-Dawley albino rats by Product Safety Labs (East Brunswick, NJ). Testing included hematology, blood chemistry, and histopathology. The procedures were in compliance with the FDA Good Laboratory Practice Regulations as set forth in 21 CFR Part 58. Flow cytometry was used to evaluate the binding of 10H3 Fab to human mononuclear cells and human red cells. Biodistribution studies were performed in BALB/C mice.

Results

Quantitative Immunocytochemistry: Comparative Activity of Intact MAb Preparations

Anti-Aβ MAbs were prepared and were classified as the gamma 2a kappa isotype. Preliminary screening indicated that MAb 10H3, which had a characteristic isoelectric focusing pattern, effectively detected senile plaques and amyloid-laden blood vessels of brain parenchyma as well as amyloidotic meningeal vessels of AD brains. Normal control brains, without amyloid deposits, were unreactive with 10H3 except for light background staining. Quantitative immunocytochemistry was carried out to compare the activity and specificity of 10H3 with other anti-Aβ MAbs obtained by the same preparative procedures. Unlike immunostained parenchymal plaques, which are comparable in numbers among serial sections of tissue, blood vessels are not uniformly distributed. Thus, quantitation of plaques in adjacent sections served as the basis for immunocytochemical assays. Multiple experiments in which each of several comparable MAbs was tested over a range of concentrations (0.1–10 μg/mL) indicated that 10H3 at a tenfold greater dilution detected as many or more plaques than other MAbs in the same series *(21)*.

Quantitative Immunocytochemistry: Activity After Fab Fragmentation

The MAbs were purified on a protein G column and enzymatically digested to Fab fragments. They retained 36–70% activity in the standard immunocytochemistry assay system *(21)*. 10H3 was then assessed relative to other comparable anti-Aβ Fab fragments by immunocytochemistry. When tested over a range of dilutions found to be effective for processing tissue (0.1–10 μg/mL) 10H3 activity was more effective than other antibodies by one log potency.

Quantitative/Qualitative Immunocytochemistry: Prelabeled and Postlabeled 10H3

Antibody 10H3 was radiolabeled with ^{99m}Tc using a bifunctional diamide dimercaptide ligand system *(see* Materials and Methods and ref. *16)*. After purification the Fabs were tested for retention of activity. By means of a quantitative dot blot procedure it was shown that the prelabeled and post-labeled Fab fragments each detected as little as 2 μg of antigen at concentration of 0.05 μg/mL (data not shown). Immunocytochemistry carried out at two antibody concentrations indicated that the number of plaques detected by the unmodified Fab fragment were comparable to values for the chelated and radio-labeled species at the effective concentrations *(21)*.

To assess retention of specificity for amyloid accumulations in the AD brain, prelabeled and postlabeled 10H3 Fab fragments were applied to AD cortex. Both before and after attachment of the diamide dimercaptide chelate of ^{99m}Tc, the Fab exhibited strong affinity for amyloid deposits in blood vessels and parenchyma without a reduction in specificity. Figures demonstrating the immunocytochemical staining properties of 10H3 MAb have been recently published *(14)*.

Toxicity, Biodistribution, and Flow Cytometry Studies

No toxic effects were demonstrated in studies in rats. Statistical evaluation of all quantitative parameters did not reveal any treatment-related effects. No binding was observed to human red cells, lymphocytes, monocytes, or polymorphonuclear lymphocytes. Both cultured monocytes and isolated human mononuclear cells from three donors showed varying degrees of binding to 10H3 Fab. The binding to cultured monocytes and isolated mononuclear cells was minimal and is speculated to be a result of the isolation procedure.

A blood clearance study in BALB/c mice showed a biphasic loss from the blood with a T1/2α = 17 min and unusually long T1/2β = 17 h (Fig. 1). Biodistribution studies at 4 and 20 h demonstrated early kidney uptake consistent with renal clearance and metabolism of Fab fragments and subsequent loss at later time points. Uptake in other organs followed blood pool disappearance (Fig. 2).

Discussion

The sequence of the Aβ (1–28) antigen used for preparation of anti-Aβ antibodies was determined from protein of amyloid plaque cores and shown to have the following sequence: N-Asp-Ala-Glu-Phe-Arg-His-Asp-Ser-Gly-Tyr-Glu-Val-His-His-Gln-Lys-Leu-Val-Phe-Phe-Ala-Glu-Asp-Val-Gly-Ser-Ser-Ala-COOH *(13)*. The unique amino acid sequence contains substitutions that distinguish it from AD amyloid peptides obtained by other procedures. When compared with the first 24 residues reported
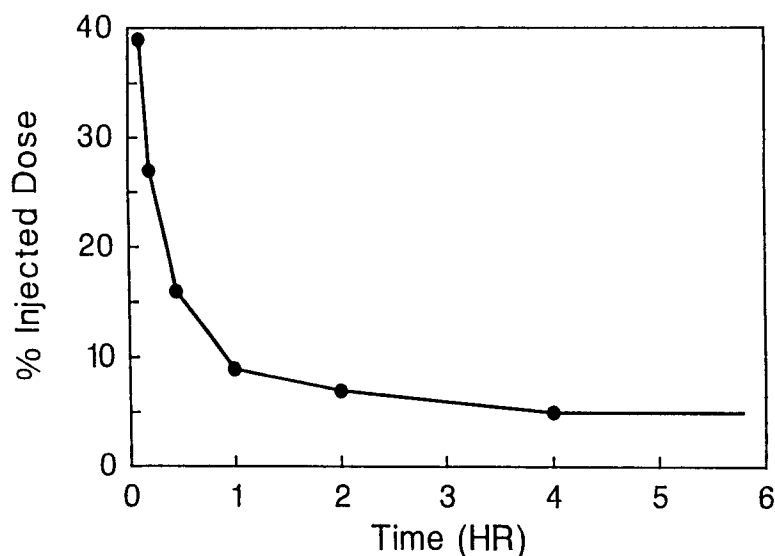
Fig. 1. Blood disappearance of ^{99m}Tc 10H3 Fab following IV administration of 10 µg in BALB/C mice ($n = 3$/ timepoint).
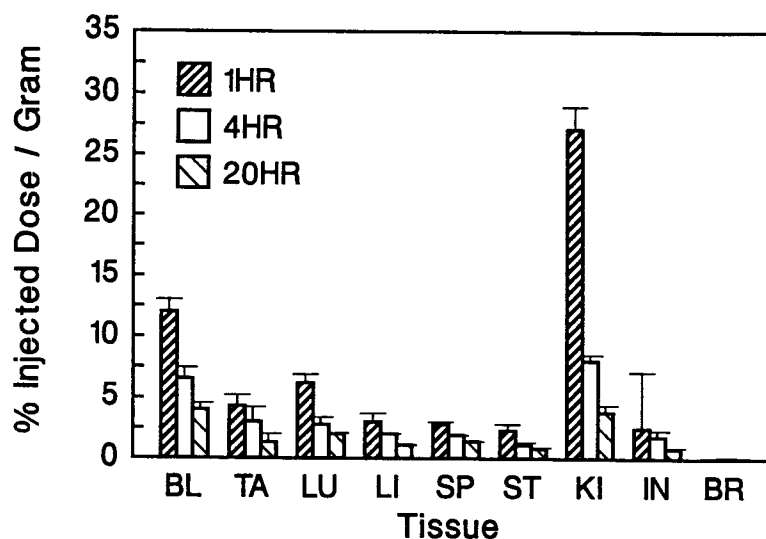

Fig. 2. Biodistribution of 10 µg ^{99m}Tc 10H3 Fab in BALB/C mice ($n = 4$/timepoint) (BL = blood, TA = tail, LU = lung, LI = liver, SP = spleen, ST = stomach, KI = kidney, IN = intestines, BR = brain).

for the corresponding peptide derived from AD brain meninges (16) Aβ (1–28) substitutes Glu for Gln at position 11. The Aβ (1–28) sequence also differs from the corresponding structure obtained by molecular cloning of APP from nondemented and AD brains (17,18); in these cases Aβ positions 27 and 28 were occupied by Asn and Lys, rather than by Ser and Ala, respectively.

Aβ (1–28) has the property of aggregating to larger species on denaturing gels (19,20). Whereas

the calculated mass is 4.2 kDa, the Aβ (1–28) sequence self assembles to additional forms that are greater than 23 kDa on denaturing acrylamide gels that contain SDS and urea (19,20). This characteristic is consistent with the reported behavior of AD amyloid peptides (21). By immunoblot procedures 10H3 was shown to react with the immunogen when it occurred both as the 4.2 Dalton denatured peptide as well as higher molecular weight aggregates (15,20).

10H3 and additional anti-Aβ MAbs reacted with parenchymal deposits of amyloid as well as the amyloid of blood vessels in the AD brain and surrounding meninges. Only pale amorphous background staining of brain tissue occurred in the absence of amyloid deposits in normal control brains. Quantitative immunocytochemistry revealed that 10H3 exhibited greater binding activity than other anti-Aβ MAbs in the same series. In other studies, double staining experiments indicated that anti-Aβ MAbs reacted with plaques and blood vessels that were also detected by thioflavin S but that the MAbs were more sensitive than the dye (15).

For radiolabeling of antibodies Fritzberg and coworkers (22) developed a diamide dimercaptide tetradentate chelating agent that allows specific and stable binding of ^{99m}Tc to proteins. The resulting product has a high degree of radiochemical purity and retains its native potency. The novel chelate was used to radiolabel antibodies with ^{99m}Tc for tumor imaging in humans using murine Fab fragments (23). The same strategy can be applied to anti-Aβ MAbs for detection of amyloid angiopathy in the AD brain. The biodistribution, flow cytometry, and toxicity studies reported here demonstrate desirable qualities for use in human studies.

It is anticipated that by this approach the diagnosis of AD by brain imaging will be feasible since the radiolabeled antibody retains high affinity and specificity for vascular amyloid, as well as for plaques. This noninvasive imaging technique may provide a means to determine the relationship of imaging evidence for AA to disease course.

Brain imaging has been a subject of extensive investigation in AD (24), but a noninvasive diagnostic method awaits development. There are currently no approaches to the assessment of the basic pathological features of the disease during life without surgical intervention. By contrast, MAbs have been widely used in the imaging and treatment of cancer (22,25–31) wherein they provide specific nontoxic markers that were shown to be safe, and, in some settings, more sensitive for tumor detection than other imaging methods. Although radioimmunodetection investigations of brain tumors in humans have been ongoing for more than 25 yr, brain diseases have received limited attention with this technique.

Our current approach takes advantage of the rapid clearance of the Fab fragment of the anti-Aβ 10H3 MAb and the exemplary properties of the ^{99m}Tc label as a diagnostic radiopharmaceutical. If successful targeting occurs, SPECT imaging may provide a noninvasive measure of AA. We do not anticipate passage of the labeled MAb through the blood–brain barrier, but expect that sites of antigen deposition on the luminal surface of the blood–brain barrier (11,12) will cause MAb binding in Alzheimer's disease brain. The absence of tight junction in the endothelium of menigeal vessels should allow for imaging of AA. Localization to intravascular Aβ deposits is expected to be less prominent in heathy aged control subjects than in AD patients. Amyloid angiopathy has not been not been quantitatively assessed throughout the brain in Alzheimer's disease. The extent and progression of AA is expected to be variable within the AD population.

A radioimmunodetection approach may allow us to assess this hypothesis, as well as attempt to correlate the severity of AA with the severity and duration of illness.

10H3 is a murine MAb to Alzheimer disease Aβ amyloid that is highly reactive and specific for blood vessel and parenchymal amyloid deposits. The MAb retained its binding characteristics after cleavage to a Fab fragment and chelation to a diamide dimercaptide tetradentate agent and labeling with ^{99m}Tc. Based on these properties, the radiolabeled antiamyloid Fab appears to be a potentially effective agent for application to the diagnosis of Alzheimer disease by in vivo imaging.

Acknowledgments

References

1. Glenner G. G., Henry J. H., and Fujihara S. (1981) Ann. Pathol. 1, 120–129.
2. Glenner G. G. (1980) N. Engl. J. Med. 302, 1283–1292.
3. Scholz W. (1938) Zeit. Neurol. Psychiat. 162, 694–715.
4. Vinters H.V. (1987) Stroke 18, 311–324.
5. Mandybur T. I. (1975) Neurology 25, 120–126.
6. Lee S. S. and Stemmerman G. N. (1978) Arch. Pathol. Lab. Med. 102, 317–328.
7. Friedland R. P. (1990) Aging of the Brain: Cellular and Molecular Aspects of Brain Aging and Alzheimer's Disease. Proceedings of the Thirteenth Teniguchi

Symposium. (Hayaishi O., Seegmiller J. E., and Nagatsu T., eds.) Tokyo: Japan Scientific Societies Press, and Basel: Karger, Basel, 147–159.

8. Ishii N., Ishihara Y., and Horie A. (1984) *J. Neurol. Neurosurg. Psychiat.* **47**, 1703–1011.

9. Ranalli P. and Bergeron C. (1984) *Ann. Neurol.* **16**, 119–127.

10. Allsop D., Landon M., Kidd M., Lowe J. S., Reynolds G. P., and Gardner A. (1986) *Neurosci. Lett.* **68**, 252–256.

11. Tomlinson B. E. and Corsellis J. A. N. (1984) in *Greenfield's Neuropathology*, 4th ed. (Adams J. H., Corsellis J. A. N., and Duchen L. W., eds.) Wiley, New York, 968,969.

12. Montjoy C. Q., Tomlinson B. E., and Gibson P. H. (1982) *J. Neurol. Sci.* **57**, 89–103.

13. Masters C. L., Simms G., Weinman N. A., Multhaup G., et al. (1985) *Proc. Natl. Acad. Sci. USA* **82**, 4245–4249.

14. Majocha R. E., Reno J. M., Friedland R. P., VanHaight C., Lyle L. R., and Marotta C. A. (1992) *J. Nucl. Med.* **33**, 2184–2189.

15. Majocha R. E., Benes F. M., Reifel J. L., and Marotta C. A. (1988) *Proc. Natl. Acad. Sci. USA* **85**, 6182–6186.

16. Kasina S., Rao T. N., Srinivasan A., Sanderson J. A., et al. (1991) *J. Nucl. Med.* **32**, 1445–1451.

17. Kang J., Lemaire J. G., Unterbeck A., Salbaum J. M., Masters C. L., Grzescmik K. H., Multhau P. G., Beyreuther K., and Muller-Hill B. (1987) *Nature* **325**, 733–736.

18. Zain S. B., Salim M., Chou W. G., Sajdel-Sulkowska E. M., Majocha R. E., Rehman S., Benes F. M., and Marotta C. A. (1988) *Proc. Natl. Acad. Sci USA* **85**, 929–933.

19. Salim M., Zain S. B., Chou W. G., Sadel-Sulkowska E. M., et al. (1988) in *Familial Alzheimer's Disease: Molecular Genetics, Clinical Prospects and Societal Issues* (Blass J. P., Miner G. D., Niner L. A., Richter R. W., and Valentine J. L., eds.), Dekker, New York, pp. 153–165.

20. Honda T. and Marotta C. A. (1992) *Neurochem. Res.* **17**, 367–374.

21. Gorevic P. D., Castano E. M., Sarma S., and Frangione B. (1987) *Biochem. Biophys. Res. Commun.* **147**, 854–862.

22. Fritzberg A. R., Kasina S., Reno J. M., Srinivasa A., et al. (1986) *J. Nucl. Med.* **27**, 957–958.

23. Eary J. R., Schroff W., Abrams P. G., Fritzberg A. R., et al. (1989) *J. Nucl. Med.* **30**, 25–32.

24. Friedland R. P. (1990) in *Handbook of Neuropsychology*, vol. 4 (Boller F. and Grafman J., eds.), Elsevier, Amsterdam, pp. 197–212.

25. Carrasquillo J. A., Krohn K. A., Beaumier P., McGuffin R. W., Brown J. P., Hellstrom K. E., Hellstrom I., and Larson S. M. (1984) *Cancer Treat. Rep.* **68**, 317–328.

26. Sands H. (1987) *J. Nucl. Med.* **33**, 29–32.

27. Divgi C. R., Welt S., Kris M., Real F. X., Yeh S. D., Gralla R., Merchant B., Schweighart S., Unger M., and Larson S. M. (1987) *J. Neurosurg.* **67**, 721–725.

28. Blasberg R. G., Makagawa H., Burdon M. A., Groothuis D. R., Patlak C. S., and Bigner D. D. (1987) *Cancer Res.* **47**, 4432–4443.

29. Fuimori K., Covell D. G., Fletcher J. E., and Weinstein J. N. (1990) *J. Nucl. Med.* **31**, 1191–1198.

30. Wilbur D. S., Hadley S. W., Hylarides M. D., Abrams P. G., Beaumier P. A., Morgan A. C., Reno J. M., and Fritzberg A. R. (1989) *J. Nucl. Med.* **30**, 216–226.